International Journal of Pharmaceutics 641 (2023) 123058

Contents lists available at ScienceDirect

International Journal of Pharmaceutics

journal homepage: www.elsevier.com/locate/ijpharm

3D printing of microencapsulated *Lactobacillus rhamnosus* for oral delivery

Pablo Rosas-Val [a,b], Masoud Adhami [c], Ana Brotons-Canto [a], Carlos Gamazo [b,e], Juan M. Irache [d,e], Eneko Larrañeta [c,*]

[a] Nucaps Nanotechnology SL, Polígono Mocholi, Vivero CEIN, 31110, Spain
[b] Department of Microbiology & Parasitology, University of Navarra, c/ Irunlarrea 1, Pamplona, 31008, Spain
[c] School of Pharmacy, Queen's University Belfast, Medical Biology Centre, 97 Lisburn Road, Belfast, BT9 7BL, UK
[d] Department of Chemistry and Pharmaceutical Technology, University of Navarra, c/ Irunlarrea 1, Pamplona, 31008, Spain
[e] Navarra Institute for Health Research (IdiSNA), Pamplona, Spain

ARTICLE INFO

Keywords:
Probiotic
Lactobacillus rhamnosus
3D printing
Microparticles
Oral delivery

ABSTRACT

3D Printing is an innovative technology within the pharma and food industries that allows the design and manufacturing of novel delivery systems. Orally safe delivery of probiotics to the gastrointestinal tract faces several challenges regarding bacterial viability, in addition to comply with commercial and regulatory standpoints. *Lactobacillus rhamnosus* CNCM I-4036 (Lr) was microencapsulated in generally recognised as safe (GRAS) proteins, and then assessed for robocasting 3D printing. Microparticles (MP-Lr) were developed and characterised, prior to being 3D printed with pharmaceutical excipients. MP-Lr showed a size of 12.3 ± 4.1 μm and a non-uniform wrinkled surface determined by Scanning Electron Microscopy (SEM). Bacterial quantification by plate counting accounted for 8.68 ± 0.6 CFU/g of live bacteria encapsulated within. Formulations were able to keep the bacterial dose constant upon contact with gastric and intestinal pH. Printlets consisted in oval-shape formulations (15 mm × 8 mm × 3.2 mm) of ca. 370 mg of total weight, with a uniform surface. After the 3D printing process, bacterial viability remained even as MP-Lr protected bacteria alongside the process (log reduction of 0.52, $p > 0.05$) in comparison with non-encapsulated probiotic (log reduction of 3.05). Moreover, microparticle size was not altered during the 3D printing process. We confirmed the success of this technology for developing an orally safe formulation, GRAS category, of microencapsulated Lr for gastrointestinal vehiculation.

1. Introduction

3D Printing is becoming an emerging technology in diverse industrial areas, including pharmaceutical and food industries (Baiano, 2022; Varghese et al., 2022). This process generates 3D objects layer-by-layer with the help of digitalized tools. It comprehends the geometry and morphology design of printlets, automatizing their manufacturing and minimising human error, thus booming both versatility and quality of formulations generated (Martinez et al., 2018; Picco et al., 2023; Zheng et al., 2020). Technological aspects such as rheology, texture and volume can be adjusted and modified, as well as dosing and drug distribution within the different layers (García-Segovia et al., 2020; Liu et al., 2019; Robles-Martinez et al., 2019). This technology enables the use of diverse matrixes and excipients, or the simultaneous incorporation of different active ingredients, increasing their stability and bioavailability (Gültekin et al., 2021; Kollamaram et al., 2018). As a result, 3D printing allows to develop personalized treatments, fitting different physiological needs and treatment dosage (Arafat et al., 2018; Awad et al., 2019; Goyanes et al., 2019; Kadry et al., 2018; Martin et al., 2021; Silva et al., 2022; Stewart et al., 2020). Therefore, specific populations could benefit from these products, such as paediatric or elderly patients with age-related dysphagia, patients with dose-adjustment treatments, as well as chronic dose-dependent pathologies (Goyanes et al., 2017; Kadry et al., 2018; Kouzani et al., 2017; Malebari et al., 2022; Pant et al., 2021).

Probiotics can be defined as "live microorganisms which, when administered in adequate amounts, confer a health benefit on the host" (Hill et al., 2014). Following oral intake, live probiotics colonize the large intestine and help normalize the human microbiota, exerting several health-promoting and disease-prevention effects (Maldonado Galdeano et al., 2019; Peng et al., 2022; Sohn et al., 2023; Yamanbaeva et al., 2023). Diverse items are commercialized upon the probiotic label, such as probiotics in food or dietary supplements, probiotic drugs, medical foods, non-oral probiotics (e.g., vaginal), probiotic for animal

* Corresponding authors.
E-mail address: e.larraneta@qub.ac.uk (E. Larrañeta).

https://doi.org/10.1016/j.ijpharm.2023.123058
Received 4 April 2023; Received in revised form 10 May 2023; Accepted 12 May 2023
Available online 18 May 2023

feed and probiotic added to infant formulas. They cover a wide variety of products with different means of administration, target populations, target sites and regulatory categories (Hill et al., 2014).

In 2022 probiotic market size was estimated to account for more than USD $2.5 billion. With an annual growth of 8%, the probiotic market share is expected to grow and surpass the number of USD $5 billion in the following years (Kunal Ahuja and Sarita Bayas, n.d.). Nevertheless, industrial development of orally safe and viable probiotic formulations faces multiple challenges, including the loss of viability during industrial manufacturing process, during long-time storage, and throughout bacterial passage along the intestinal tract after oral administration. Therefore, multiple techniques for probiotic vehiculation have been developed with the aim to protect them (Terpou et al., 2019). Microencapsulation in organic particles with Generally Recognized As Safe (GRAS) category comes up as an innovative solution to fulfil the needs of the nutraceutical industry.

Previous works have tried to develop probiotic products based on 3D printing technology. Liu et al. (2020) 3D printed *Bifidobacterium animalis* subsp. *Lactis* in mashed potatoes, while Dodoo and collaborators (Dodoo et al., 2020) ink-jetted a *Streptococcus salivarius* strain in oro-dispersible films with xylitol. In another interesting work, *Lactobacillus plantarum* were incorporated in a hydrogel, prior to be printed within a symbiotic-composite flour construct (Yoha et al., 2021). In a similar way, a 3D printed hydrogel formulation with *Bifidobacterium lactis* and *Lactobacillus acidophilus* was also developed by Kuo et al. (2022), while Xu et al. (2023) 3D printed *B. lactis* in a gel stabilized by tea protein/xanthan gum. Most of them observed a protective effect upon bacterial viability after the 3D printing process, which could be attributed to the matrix where probiotics were embedded and/or encapsulated within, reaching >log 6 CFU/g in the final product. Nevertheless, no previous work with microencapsulated probiotics generated by desolvation, GRAS protein-based, has been developed so far.

The aim of this study was to develop a microencapsulated probiotic formulation based on robocasting 3D-printing technology, for oral delivery, ensuring the delivery of a specific dose of live bacteria in the large intestine to achieve the desired biological effect. For this purpose, a strain of *L. rhamnosus* CNCM I-4036 (Lr) was cultured and then microencapsulated in casein based microparticles. Physicochemical characterization of probiotic loaded microparticles (MP-Lr) such as size and morphology were studied. Encapsulation efficiency and gastrointestinal resistance were performed as well. Afterwards, printlets were generated with a 3D printing method based on extrusion. The probiotic printlets (3D-MP-Lr) obtained were assessed for morphology, thermal and infrared analysis, mechanical strength and weight variation, disintegration time and, finally, for bacterial quantification and viability.

2. Materials and methods

2.1. Materials

MRS Broth and Agar were supplied by Condalab (Spain). Sodium caseinate was provided by ACROS Organics (France). Chitosan and mannitol were obtained from Guinama (Spain). Dipotassium phosphate (KH_2PO_4), pepsin, pancreatin, and trypsin were provided by Sigma-Aldrich (USA). HCl 37 %, NaCl, NaOH and sucrose were supplied by PanReac AppliChem ITW Reagents (Spain). Plasdone™ K-29/32 (poly (vinylpyrrolidone), PVP, Mw 58 kDa) was purchased from Ashland (USA). Glycerol (reagent grade ≥99.5%) was provided by AnalaR NORMAPUR® ACS (VWR Chemicals BDH®, USA). PBS (pH 7.4 ± 0.05; 0.14 M NaCl, 0.003 M KCl, 0.01 M PO_4^{3-}) and PBS-Tween (pH 7.4 ± 0.05; 0.14 M NaCl, 0.0027 M KCl, 0.01 M PO_4^{3-}, 0.05% Tween™ 20) were supplied by Medicago (Sweden).

2.2. Preparation of microparticles

2.2.1. Bacterial culture

Lr was kindly provided by Biopolis S.L.-ADM (Spain). A sub-culture was grown in MRS Broth (Condalab, Spain) at 37 °C for 24 h under microaerophilia, with constant shaking (100 rpm). Then, a 1% v/v was inoculated in a bioreactor (Infors HT, Switzerland) and monitored with the bioprocess control software Eve® (Infors HT, Switzerland).

2.2.2. Microencapsulation

Empty (MP) and probiotic loaded (MP-Lr) microparticles were prepared based on the principle of desolvation. The matrix solution was prepared as described in the WO20140062621 patent, property of Nucaps Nanotechnology S.L (Agüeros et al., 2013).

Bacterial cells were collected by centrifugation at 10,000*g* for 15 min and washed twice with a sucrose solution (2% w/v). About 1.5 mL of the bacterial suspension were added to a 25 mL of an aqueous solution of sodium caseinate (10 mg / mL). Subsequently, on the mixture, 10 mL of a chitosan solution of concentration 1.6 mg / mL prepared in aqueous medium with pH 5.5–6 was added (pH adjustment with 0.1 N HCl). After five minutes of incubation, 1 mL mannitol (100 mg/mL) was added to the mixture above. MP preparations were prepared following the same methodology, but for the addition of bacteria.

Microparticles were collected by spray-drying in a Büchi Mini Spray Drier B-290 apparatus (Büchi Labortechnik AG, Switzerland). The parameters selected were the following: inlet temperature of 100 °C, spray-flow of 600 mL/h, and aspiration rate at 100% of the maximum capacity.

2.3. Characterization of microparticles

2.3.1. Size & distribution

Particle size and size distribution of MP and MP-Lr were determined by laser diffractometry. Samples were diluted in deionized water, at 25 °C, and then measured with a Mastersizer-S® (Malvern Instruments, UK). Size is indicated as the surface area mean (Sauter Mean Diameter; $D_{[3,2]}$) (Kowalczuk and Drzymala, 2016).

2.3.2. Morphology

Shape and surface of MP-Lr were examined by scanning electron microscopy (SEM). For this purpose, samples were prepared as described in Section 2.2.2., mounted on SEM grids (glass plates adhered with a double-sided adhesive tape onto metal stubs and dried) and left overnight to dry. Then, samples were coated with a gold layer using a Quorum Technologies Q150R S sputter-coated (QuorumTech, Canada), and analysed using a Sigma 300 VP microscope equipped with a GEMINI® Field-Effect SEM column (ZEISS, Germany) operating between 1 and 3 kV.

2.3.3. Bacterial quantification

To estimate the viable bacteria within the microparticles, 40 mg of the dried MP-Lr powder was accurately weighed in an analytical balance (Mettler Toledo, Spain) and dispersed in 5 mL PBS. Then, 1 mL of a trypsin solution (1 mg/mL) was added to the formulation and left incubated at 37 °C for a 1 h under magnetic stirring. Decimal dilutions in PBS-Tween 20 and seed were performed. After incubation at 37 °C under microaerophilic conditions for 48 h in MRS Agar, CFU counts were performed. Bacterial death cycles were determined using the following equation:

$$\text{Bacterial death cycles} = \text{Log (initial CFU/g)} - \text{Log (recovered CFU/g)}$$

in which the Log (initial CFU/g) was the number of bacteria initially included in the preparative process per gram of formulation, and Log (recovered CFU/g) represented the counts of viable bacteria obtained at the end of the preparative process of MP-Lr.

2.3.4. Stability & storage

Bacterial viability during storage alongside time was studied. Free atomized *Lr* and MPLr were kept under aerobic conditions at (i) room temperature, (ii) at 4 °C and (iii) within a hermetic container at 4 °C with a silica gel humidity-saturation indicator system (RS PRO, France).

Samples were kept under the above-mentioned conditions up to 12 months. Bacterial quantification was performed at several time points as described in Section 2.3.3.

2.3.5. Gastrointestinal resistance

The gastrointestinal (GI) resistance of MP-Lr was tested as described elsewhere (Vinderola and Reinheimer, 2003), with some minor modifications. Simulated gastric (SGF) and simulated intestinal (SIF) fluids were freshly prepared before each experiment, according to the European Pharmacopeia (Ph. Eur., 9th Ed). For SGF, 2 g NaCl and 3.2 g pepsin from porcine gastric mucosa were dissolved in 7 mL HCl and a sufficient volume of sterilized water to make 1 L. The pH of SGF was fixed to 1.2 ± 0.1, and the solution was filtered by 0.22 μm sterilized filter (Millex-GV, Millipore, USA). For SIF, 6.8 g KH_2PO_4 and 10 g of pancreatin from porcine pancreas were dissolved in water up to 1 L. The solution was then adjusted to pH 6.8 ± 0.1 and filtered by 0.22 μm sterilized filter.

A specific amount of MP-Lr was weighed and incubated for 0.5, 1 or 2 h in gastric medium at 37 °C in an orbital shaker at 1,000 rpm in three replicates. Non-encapsulated atomized bacteria were used as control. Then, samples were extracted at each time point for viable count analysis. Samples were centrifuged at 10,000*g* for 10 min and the supernatant was removed, whereas the pellets were. washed twice with saline solution, and viable bacteria count was performed by plate counting.

The fraction of surviving bacteria was calculated as follows:

$$\text{Log survivor fraction} = \log N_t - \log N_o.$$

where N_t represents the total viable bacteria after each time of treatment, and N_o the initial number of inoculated bacteria.

For evaluating intestinal resistance, after being incubated 2 h in SGF, samples were centrifuged at 10,000*g* for 10 min and the supernatant was removed. The pellet was washed twice with saline solution, before adding SIF. Samples underwent 0.5, 1 or 2 h with the SIF and under constant shaking, prior to being analysed by plate counting as described in Section 2.3.3.

2.4. Design and manufacture of 3D probiotic printlets

Blank (3D-MP) and probiotic printlets (3D-MP-Lr) formulations were comprised of a specific mixture of PVP (55%), Glycerol (5%) and MP or MP-Lr (40%), respectively. The formulation was mixed using a SpeedMixer™ DAC 150.1 FVZ-K (Hauschild GmbH & Co. KG, Germany) at 3,500 rpm for 2 min, to facilitate their printing. Then, mixtures were loaded into a 10 mL plastic syringe with a 0.8 mm gauge tip which was then attached to the 3D printer head as described elsewhere (Utomo et al., 2023). Computer-aided design (CAD) software was used to prepare the printlets. Each printlet took <3 min to be printed.

Then, formulations were printed at ambient lab conditions by extrusion-based technology using a Bioscaffolder 3.2. (GeSiM, Germany) robocasting 3D-printer and monitored with GeSiM Robotics software (GeSiM, Germany). The printer was set with printing speed of 5 mm/s and temperature of 24 °C. The strand distance was set at 0.6 mm and nozzle pressure was 300–400 kPa. Upon printing completion, printlets were dried in a fume hood under ambient lab conditions for 2 days. As a bacteriological control, non-encapsulated *Lr* was printed following the same procedure (3D-Lr), to assess the effect of 3D printing on bacterial viability. Formulation was comprised of a mixture of PVP (90%), glycerol (5%) and bacterial cells (5%), respectively.

2.5. Characterization of printlets

2.5.1. Printlets morphology

Morphology, shape, and surface of printlets were examined by optical microscopy and SEM. Optical microscopy was performed with a Leica EZ4 D light microscope (Germany), and SEM with a Tabletop Hitachi TM3030 microscope (Japan).

2.5.2. Printlets thermal analysis

The response of the different microparticles to temperature changes was studied by differential scanning calorimetry (DSC). The variations in the functional groups of the printlets were analysed with a Q20 Differential Scanning Calorimeter (TA instruments, Bellingham, WA, USA).

The DSC studies of the different samples were carried out by accurately weighing a small portion (between 5 mg and 10 mg), followed by placing and sealing the aluminium pans. A sealed, empty aluminium pan was used as a reference. At a temperature range from 20 to 300 °C, operated under a nitrogen flow rate of 50 mL/min and with a heating rate of 10 °C/min.

2.5.3. Printlets infrared spectroscopy

The attenuated total reflectance (ATR) approach was performed with Nicolet™ iS50 ATR (Thermo Scientific™, USA). The spectra were collected with a resolution of 4 cm^{-1} and spanned the range of 4,000 cm^{-1} to 600 cm^{-1} at 32 scans.

2.5.4. Printlets mechanical strength

A hardness tester TBH 125 (Erweka, Germany) was used to determine the mechanical strength (breaking force) of the three randomly picked printlets and the values were recorded in N (Newtons) units. The printlets were placed in the hardness tester machine on their longest axis.

2.5.5. Printlets weight variation

Up to ten 3D-MP and ten 3D-MP-Lr were individually weighed in an analytical balance (Mettler Toledo, Spain). Their average weight and standard deviation were estimated.

2.5.6. In vitro disintegration testing

Disintegration studies were carried out using the USP disintegration apparatus. Six randomly picked printlets were placed in the basket of DTG 1000 (Copley Scientific, UK) disintegration apparatus, and shaken in an upward and downward direction (30 cycles/min) for an hour in 1L of deionized water at 37 °C. The experiment was continued till the printlets completely disintegrated, and the time was recorded.

2.5.7. Bacterial viability

Bacterial viability after 3D printing procedure was evaluated. For this purpose, three 3D printlets (loaded with Lr or MP-Lr) were weighed and dissolved in PBS, left for incubation at 37 °C at 250 rpm under magnetic stirring until complete dissolution. Then, bacterial quantification was performed as described above in Section 2.3.3.

2.6. Statistical analysis

All statistical analyses and graphical representations of the data were performed using GraphPad Prism 8 software (Graphpad Software Inc., USA). Means and standard errors were calculated for every data set. The physicochemical characteristics of microparticles and printlets, as well as the *in vitro* studies were compared using the Student's *t*-test.

3. Results and discussion

3.1. Microparticles characterization

Table 1 summarizes the physicochemical characteristics of MP and

Table 1
Physicochemical characteristics of empty (MP) and probiotic loaded (MP-Lr) microparticles. Data expressed as mean ± SD (n > 3).

	Size (μm)	CFU/g
MP	10.2 ± 1.9	–
MP-Lr	12.3 ± 4.1	8.68 ± 0.6

MP-Lr. Encapsulation of probiotics barely affected particle size when compared with empty microparticles (12 μm vs. 10 μm, respectively) ($p > 0.05$). Fig. 1 compares free and encapsulated bacteria, the latter included within a spheric microparticle with a coarse, wrinkled and non-uniform surface. The appearance of these microparticles is consistent with previously reported casein microparticles for probiotic bacteria encapsulation where the bacteria was disperse within the protein matrix (Peñalva et al., 2023).

Bacterial quantification showed a final concentration of 8.68 ± 0.6 CFU/g of live bacteria in the MP-Lr powder (Table 1). These values are in line with the values obtained for probiotic products available in the market (Fiore et al., 2020; Stasiak-Różańska et al., 2021; Zawistowska-Rojek et al., 2022). Moreover, the doses are in line with the doses assumed to exert a biological effect (Fonollá et al., 2019; Lundelin et al., 2017; Sanchez et al., 2014; Slykerman et al., 2017).

Fig. 2 shows viability data of bacterial probiotic (initial concentration of log 9 CFU/g) alongside storage. When comparing free against encapsulated bacteria, the encapsulation contributed to keep the dose constant for a longer period of time in all testing conditions, protecting bacteria within. Storage upon refrigerating conditions contributed to extend viability alongside time, while the addition of a humidity-control system resulted in a slightly increase of viability.

Fig. 3 shows the gastrointestinal resistance profile of MP-Lr and non-encapsulated atomized *Lr*. The encapsulation protected bacteria from the deleterious effect of gastric pH by keeping a constant dose of viable bacteria after being 2 h in contact with pH 1.2. Non-encapsulated atomized *Lr* experienced a complete reduction in viability after 0.5 h in contact with pH of 1.2. Intestinal pH did not affect bacterial viability.

3.2. Probiotic printlets characterization

3D-printlets were successfully prepared using the formulations described in the material and methods section. The first formulation that was tested contained only PVP. However, printlets showed cracks during the drying process (data not shown). Therefore, glycerol was added as a plasticiser to avoid this issue. Printlets outer dimensions were 15 mm length × 8 mm width × 3.2 mm height, with an oval shape (Fig. 4). These dimensions are in line with previously described printlets for oral drug administration (Khaled et al., 2018b, 2018a). The morphology of the printlets reveals a rough surface due to the combination of layer height and nozzle size selected in this study. Using smaller nozzles and increasing the layer height will render smoother printlets but this will significantly increase the printing time. This is important to consider as using the parameters described here each printlet takes 2–3 min to be prepared. Besides macroscopically akin, weight average revealed that 3D-MP printlets were lighter than 3D-MP-Lr (292 mg vs. 371 mg, respectively) ($p < 0.05$) (Table 2**).** These results suggest that the presence of the MP-Lr affects the printing process. The quantities of MP and MP-Lr used to prepare the printlets were equivalent. Therefore, the difference in printlet weight can be due to difference in viscosity or density of the overall. Moreover, MP content and the probiotic bacteria dose per printlet can be seen in Table 2.

Table 2 shows the hardness values obtained for 3D-MP and 3D-MP-Lr. The equipment used to record hardness records fracture force of tablets. 3D-MP were soft and they did not show a clear fracture force. Therefore, no fracture force was recorded. These tablets were compressed without breaking. On the other hand, 3D-MP-Lr showed a clear fracture force of ca. 170 N.

Disintegration time is critical for oral tablets to release their cargo within the gastrointestinal tract. The disintegration time of the printlets prepared for this study is presented in Table 2. 3D-MP showed shorter disintegration times than printlets containing *Lactobacillus rhamnosus* ($p < 0.05$). Further imaging analysis by SEM showed slight differences regarding shape, morphology and surface between 3D-MP and 3D-MP-Lr, the former displaying a smoother surface (Fig. 5). It is important to note that in all cases the printed layers were fused together and that no accumulation of material or crystals were observed. These images suggest that the excipient and MPs are well dispersed within the printlet.

Printlets were characterised by using FTIR and DSC (Fig. 6). FTIR spectra of caseinate shows typical IR peaks reported previously for this protein (Pan et al., 2013; Zhao et al., 2018). These peaks can be attributed to the amine groups (1,600–1,700 and 1,510–1,530 cm^{-1}). These peaks can be found in MP and MP-Lr formulations as these formulations contain sodium caseinate. Additionally, these formulations contain mannitol and characteristic peaks (ca. 3,400 cm^{-1} for OH stretching and ca. 1,280 cm^{-1} for OH deformation) (Bruni et al., 2009). These formulations contained chitosan but the amount of this compound loaded into the MP formulations was too low to see any representative peaks in the FTIR spectra of the MP formulations. It can be seen that the FTIR spectra of MP and MP-Lr are a combination of the mannitol and sodium caseinate.

On the other hand, printlets display these previously mentioned peaks and PVP carbonyl peak at around 1650 cm^{-1} (Tekko et al., 2020). Interestingly, as can be seen in Fig. 6B 3D-MP and 3D-MP-Lr displayed a sharp peak at around 1650 cm^{-1} that does not match with the sodium

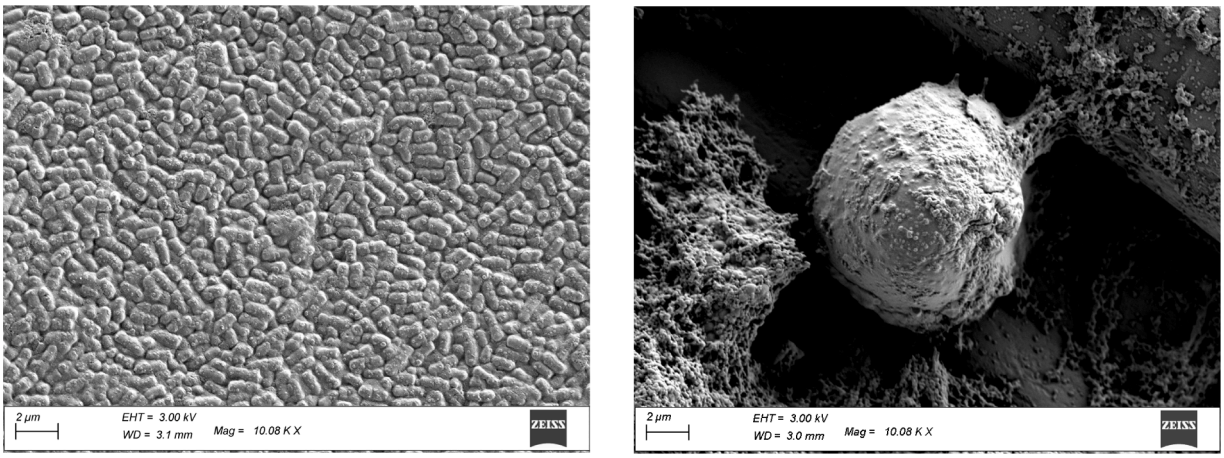

Fig. 1. Scanning Electron Microscopy (SEM) of (A) free and (B) encapsulated *Lr*.

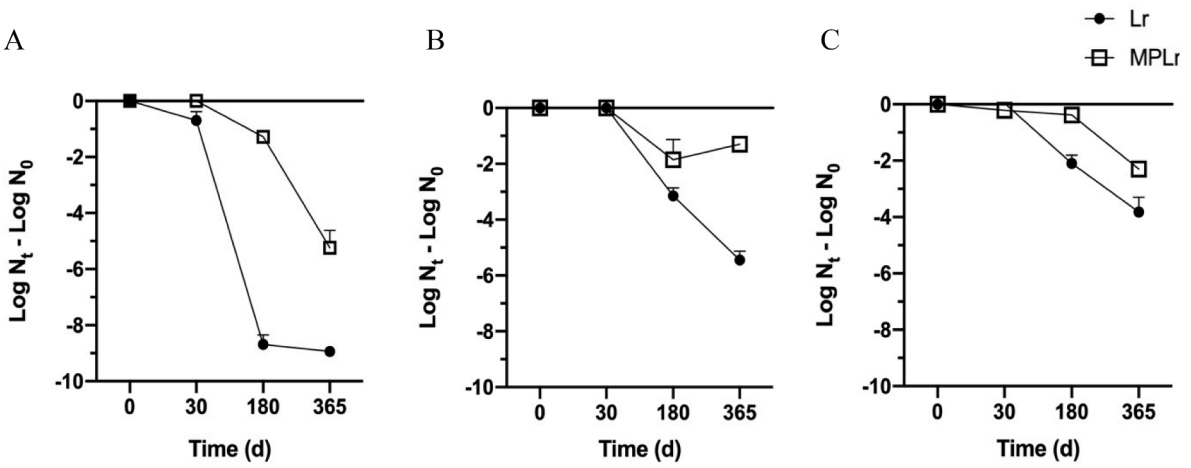

Fig. 2. Viability of free and encapsulated *Lr* over time, upon different storage conditions. Bacterial viability data is summarized at different times (1, 3, 6 and 12 months), under aerobiosis storage and at different conditions: (A) room temperature, (B) 4 °C and (C) 4 °C with humidity control within a hermetic container. Data expressed as mean ± SD (n > 3). Lr: free atomized *L. rhamnosus*; MPLr: encapsulated *L. rhamnosus* in casein-chitosan microparticles.

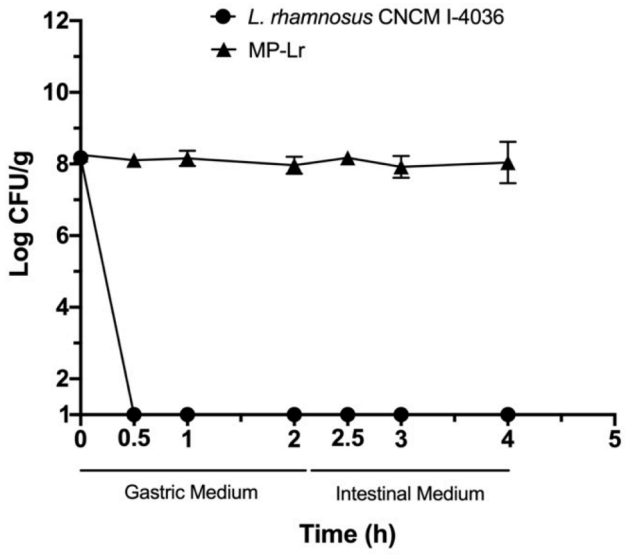

Fig. 3. In vitro comparison of gastrointestinal resistance of *Lr* non-encapsulated vs. encapsulated. Reduction in bacterial concentration alongside time are shown, upon contact with Simulated Gastric Fluid (SGF) (0.5, 1 or 2 h) and Simulated Intestinal Fluid (SIF) (2.5, 3 or 4 h). Data are expressed as Mean ± SD (n > 3).

caseinate or PVP peak. Due to the larger quantity of PVP in the printlet formulation this peak can be attributed to PVP carbonyl. Moreover, PVP is interacting with the MP formulations as it shows a peak shift for the carbonyl to lower wavenumbers indicating a potential hydrogen bond (Kuo and Chang, 2001).

Fig. 6C shows the DSC curves for the formulations developed in this work. It can be seen that PVP and casein shows water loss between 50 and 125 °C (Chan et al., 2015; Sun et al., 2016). On the other hand, mannitol shows a fusion peak at around 170 °C (Munir et al., 2022). Interestingly, mannitol fusion peak can be found in both MP formulations. However, the peak is broader and has shifted to lower temperatures. This indicates a lower degree of crystallinity for this compound. Interestingly, this peak cannot be observed in the printlet formulations for 3D-MP-Lr while a small mannitol fusion peak can be seen for 3D-MP.

Table 3 gathers bacterial quantification results. 3D printing procedure did not affect bacterial viability when encapsulated. MP-Lr protected bacteria alongside the process, and dose was kept even before and after printing ($p > 0.05$). Non-encapsulated *Lr* was affected by the process itself, resulting in a diminution of up to 3 logs ($p < 0.05$). These results indicate that the encapsulation process is critical to ensure bacterial viability during the printing process. Without encapsulation bacterial viability is reduced during the printing and drying process. Additionally, the particle size was measured after the printing process for 3D-MP-Lr obtaining particle sizes of 15.5 ± 1. These results indicate that there was no significant difference between the particle size of the initial formulation and the re-dispersed formulation after the 3D-printing process ($p > 0.05$).

4. Discussion

Pharmaceutical, food and nutraceutical industry have experienced a revolutionary spike in the research and development area. Multiple patents and innovative products turn up in the market every year, introducing new technologies. The current technological and scientific milestone enables the development of new products that look after consumers' necessities and demands. In the health scene, multiple approaches have arisen to fulfil consumers' health consciousness. Functional foods cover a wide variety of products containing substances or live microorganisms with a positive impact in human health and preventing disease, at a suitable concentration (Temple, 2022).

This work evaluates the use of 3D-printing technologies for the preparation of printlets containing *Lr*. The *Lactobacillus* genre has a wide history within the food and nutraceutical industry (Dioso et al., 2020; Patro et al., 2016; Ullah et al., 2019; Vecchione et al., 2018), due to the multiple health effects they exert upon the gastrointestinal and immune health (Dou et al., 2021; Mazziotta et al., 2023; Szajewska et al., 2013; Wang et al., 2023). However, not every probiotic strain nor dosing can exert a biological effect upon the host (Hill et al., 2014).

Isolated from faeces of exclusively breast-fed infants, the CNCM I-4036 strain showed the ability to adhere to HT-29 cells and to inhibit the growth of enteropathogens such as *Escherichia coli*, *Listeria monocytogenes*, *Salmonella* and human rotavirus (Muñoz-Quezada et al., 2013a, 2013b). The strain also showed the ability to activate Toll-like Receptor 2 and 4 in dendritic cells challenged with *E. coli* (Bermudez-Brito et al., 2014). A clinical study performed by Plaza-Diaz et al. in healthy volunteers confirmed the safety of the *Lr*, as well as its immunomodulatory profile: daily administration of the strain increased the percentage of regulatory T lymphocytes and decreased the TNF-α/IL-10 ratio, showing an anti-inflammatory effect (Plaza-Diaz et al., 2013).

In order to confer a health benefit, probiotics must remain unaltered both during storage and during transit throughout the intestinal tract,

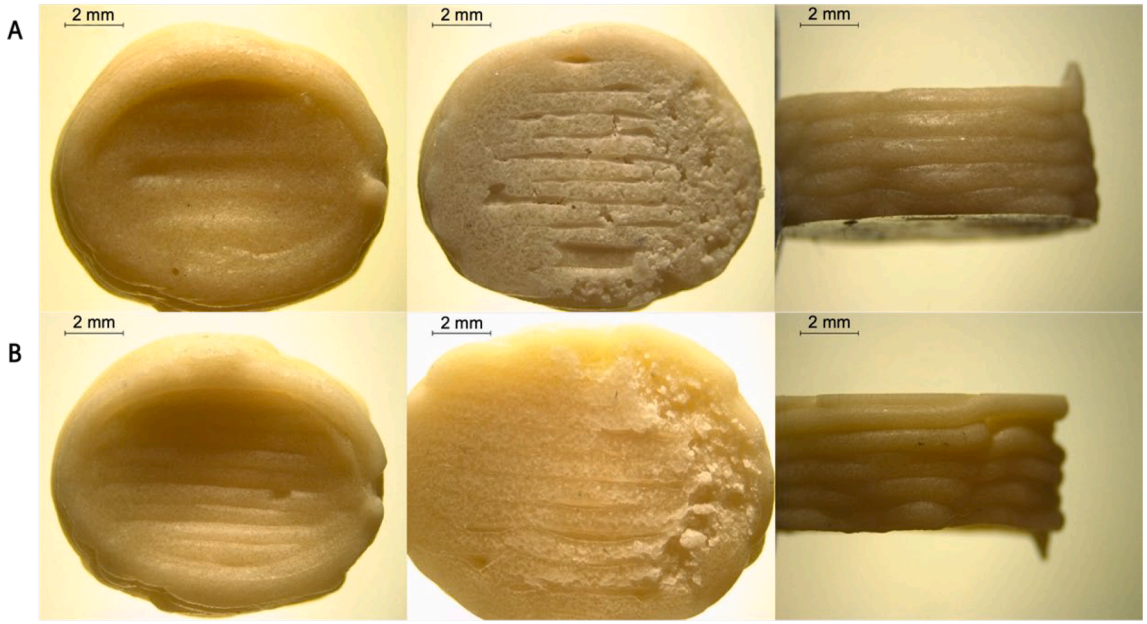

Fig. 4. (A) Blank and (B) probiotic-loaded microparticle printlets visualized by optical microscopy, from different angles and sides.

Table 2
Main characteristics of blank (3D-MP) and Lr loaded microparticles (3D-MP-Lr) printlets. Data expressed as mean ± SD (n > 3).

	Weight (mg)	MP content (mg)	Lr content (log CFU/g)	Hardness (N)	Disintegration time (min)
3D-MP	292 ± 21	112 ± 18	–	–	37 ± 6
3D-MP-Lr	371 ± 21	148 ± 33	7.86 ± 0.03	172 ± 21	45 ± 5

after oral administration (Hill et al., 2014; Terpou et al., 2019). As mentioned before, many commercial probiotics fail to achieve the aforementioned. For that reason, many manufacturers overfill their products with additional microbial cells, reaching $\geq 10^{10}$ UFC/g of product, with a significant increase in the costs of production (Fiore et al., 2020). Moreover, commercialized probiotic products are mainly freeze-dried. Freeze-drying presents several drawbacks, highlighting the high cost in terms of time and energy, since it is a non-continuous process. In addition, a second grinding stage is required to convert the freeze-dried product into a loose, micronized powder, easy to handle or incorporate into other matrices for easy storage, transport and consumption (Santivarangkna et al., 2008). Likewise, cell viability is conditioned by the process parameters: the freezing rate is crucial in preventing cell damage caused by mechanical and osmotic stress. Therefore, standardizing the criteria for probiotic freeze-drying is difficult as the optimal freezing rate is strain-dependent (Sang et al., 2023; Wang et al., 2020).

Naissinger da Silva et al. characterized the effect of gastric medium on 11 commercial probiotic formulations: after contact with the simulated gastric medium, only 6 formulations showed counts above log 6 CFU/g. It is worth mentioning that at the time of analysis, all of the commercial formulations showed bacterial counts different from what was stipulated in the labeling (Naissinger da Silva et al., 2021). Residual probiotic counts may not be sufficient to exert beneficial health effects, as the probiotic effect is strongly dose-related (FAO/WHO, 2006; Hill et al., 2014).

We showed in the present work that viability of the probiotic strain *Lr* decreased after a 12-months storage upon different conditions, such as temperature and humidity (Fig. 2). Moreover, the strain could not survive the harsh conditions of the gastrointestinal tract after 30 min in contact with simulated gastric fluid (Fig. 3). To overcome these limitations, *Lr* was encapsulated into casein-based microparticles. When compared with free bacteria, microencapsulation kept probiotic dose unaltered after storage up to 12 months, upon different conditions of temperature and humidity. Moreover, dosing was even after probiotic-loaded microparticles faced 2 h of contact with gastric and intestinal simulated fluids, consecutively (Fig. 2). Long term stability was not performed for the encapsulated bacteria loaded into the printlets as one of the purposes of 3D-printing is to prepare on demand formulations adapted to patient's needs, so they do not require long-term storage. However, stability of the encapsulated bacteria is critical so it can be stored at the point-of-care for prolonged periods of time to production of customised formulations for patients.

Technologies for the microencapsulation of probiotics are wide and diverse. However, many fail to surpass the legislative requirements for their commercialisation and, therefore, access to consumers (Vivek et al., 2023). There are few examples of commercialised products that include microencapsulated probiotics, such as Probiocap® (Lallemand Inc, 2023) or Duaolac® (Cell Biotech., 2023). Nevertheless, *Lr* is not available in that form.

The FDA and EMA have prepared a regulatory framework for microencapsulated probiotic bacteria. However, the use of 3D-printing for food and pharmaceutical applications has been currently explored and, therefore, there are still several unanswered regulatory questions, such as quality assurance. However, studies have been conducted safely in hospitals with patients treated with 3D-printed formulations (Goyanes et al., 2019). These results suggest that this technology could be translated into clinical setting soon after addressing some regulatory challenges.

The formulation developed in the present work is composed of reagents with GRAS category and, thus, complies with the legislative requirements for its commercialization for human consumption. In the European Community, strains of the genus *Lactobacillus* spp. have a long history of commercialization in the food and nutraceutical industry, being considered safe for human consumption. Nowadays, products marketed with the strain *Lr* can be found (Gasteel®, Gasteel Kids®, Gasteel Plus®) by Laboratorios Heel España, S.A.U. (Heel España,

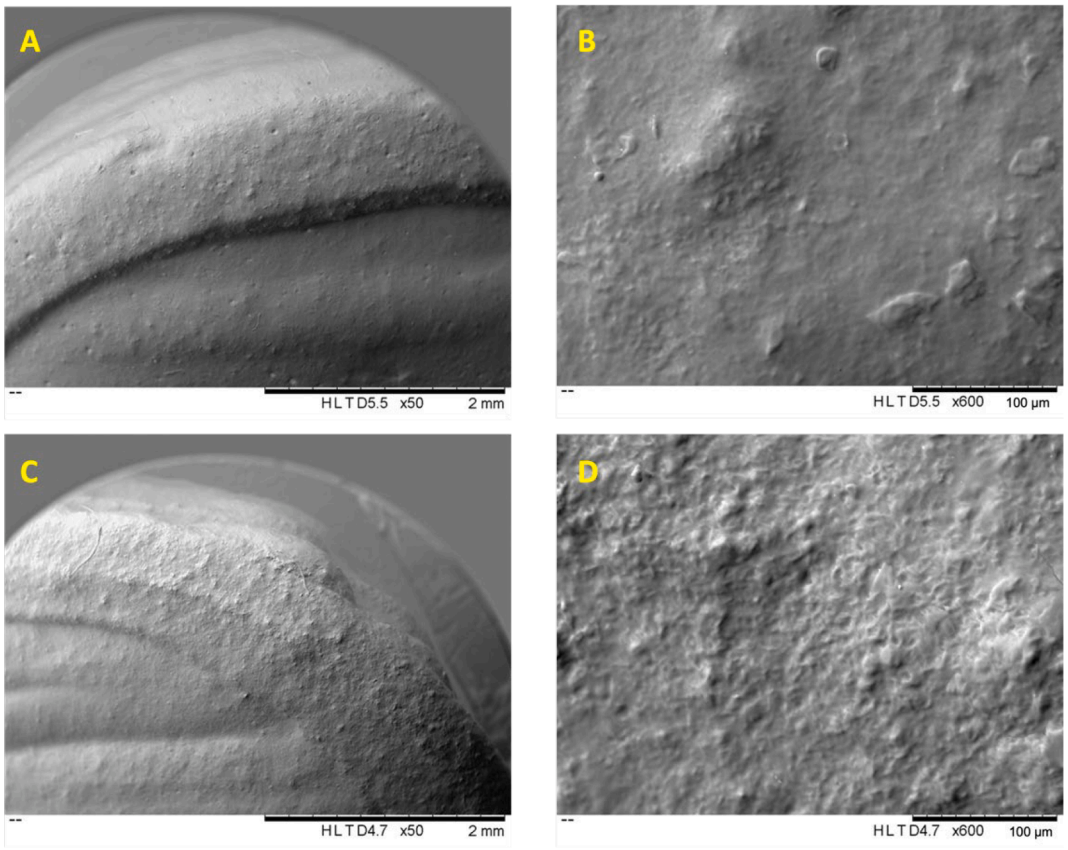

Fig. 5. Scanning Electron Microscopy (SEM) of (A, B) blank and (C, D) *Lr* loaded-microparticles printlets, with a magnification comparison.

2023), demonstrating its safety for oral use. However, none of them are encapsulated.

The microparticle formulations presented here comes up as an innovative solution: it offers the ability to deliver an already tested probiotic strain in the gastrointestinal tract, at the desired dose and up to 12 months, without the drawbacks and costs of overfilling with additional cells or freeze-drying. 3D printlets developed in the present work can deliver a dose of ca. log 7 CFU. Probiotic effect is dose-related; therefore, further studies should be carried to confirm that biological effect derived from delivery of log 7 CFU/printlet is comparable to non-encapsulated commercial alternatives (>log 10^{10} CFU/g of product).

Food proteins have been used extensively for encapsulation purposes as they are safe and highly available (Can Karaca et al., 2015; Peñalva et al., 2019; Penalva et al., 2015; Quintero Quiroz et al., 2020). Moreover, the formulations developed in this work were formulated into pastes containing pharmaceutical approved excipients. These formulations were used to prepare printlets loaded with *Lr* using a robocasting-based 3D-printing technique.

To the best of our knowledge this is the first report of a 3D-printing method to produce printlets containing *Lactobacillus rhamnosus*. Robocasting was the type of 3D-printing selected for this study to prepare Lr-loaded printlets. This technique is the ideal technique to prepare cell/bacterial containing materials as it used concentrated formulations or gels and do not require high temperature that can damage the cargo. Other printing technologies such as fused deposition modelling or selective laser sintering are not suitable for this purpose as they require high temperature. On the other hand, stereolithography does not require higher temperatures but it uses resins and potentially toxic photo-initiators. On the other hand, all these techniques present higher resolution than robocasting and the printing parameters are easier to optimise.

As mentioned before, 3D-printing is proposed as an ideal method to prepare probiotic bacteria loaded printlets at the point of care. Probiotic bacteria have been used to treat and prevent different conditions such as GI tract infections, atopic dermatitis, inflammatory bowel disease or irritable bowel syndrome (Cukrowska et al., 2021; Segers and Lebeer, 2014). The use of 3D-printing can be used to automatically adjust the dose as the dose of probiotics depends on specific disease (National Institute of Helath, 2022). 3D-printing can be especially useful in hospital pharmacies to prepare patient specific formulations in an automated way minimising human mistakes during preparation. This is even more important considering that the potential patients treated with this type of formulations include elderly and paediatric patients that could require adapting not only the dose but the size and/or shape of the printlet. The feasibility of this approach has been previously demonstrated in a clinical trial by Goyanes et al. (2019). Finally, it is important to mention that the advantages of 3D-printing dosage forms are combined with the advantages of encapsulated probiotic bacteria that offer a higher stability within the GI tract while modify the distribution maximising the targeting to distal small intestine and colon (Peñalva et al., 2023) where the main therapeutic site of action (Prakash, 2008).

The results presented here suggest that this technique can be successfully used to prepare well-formed printlets. The resulting printlets were characterised by evaluating their weight, hardness and disintegration kinetics. Finally, FTIR and DSC were performed. The results suggested that each printlet contained an average of log 7 CFUs of *Lactobacillus rhamnosus*. These results suggest that 1 printlets will be required to achieve the recommended dose of the probiotic bacteria (Fiore et al., 2020; Hill et al., 2014; Stasiak-Różańska et al., 2021; Zawistowska-Rojek et al., 2022). Previous works reporting 3D-printing of probiotic bacteria have focused on printing hydrogels (Kuo et al., 2022; Xu et al., 2023; Yoha et al., 2021) and not defined dosage forms. In this way, the relevant dose of probiotic bacteria can be adjusted to patient's needs in an easy and convenient dosage form.

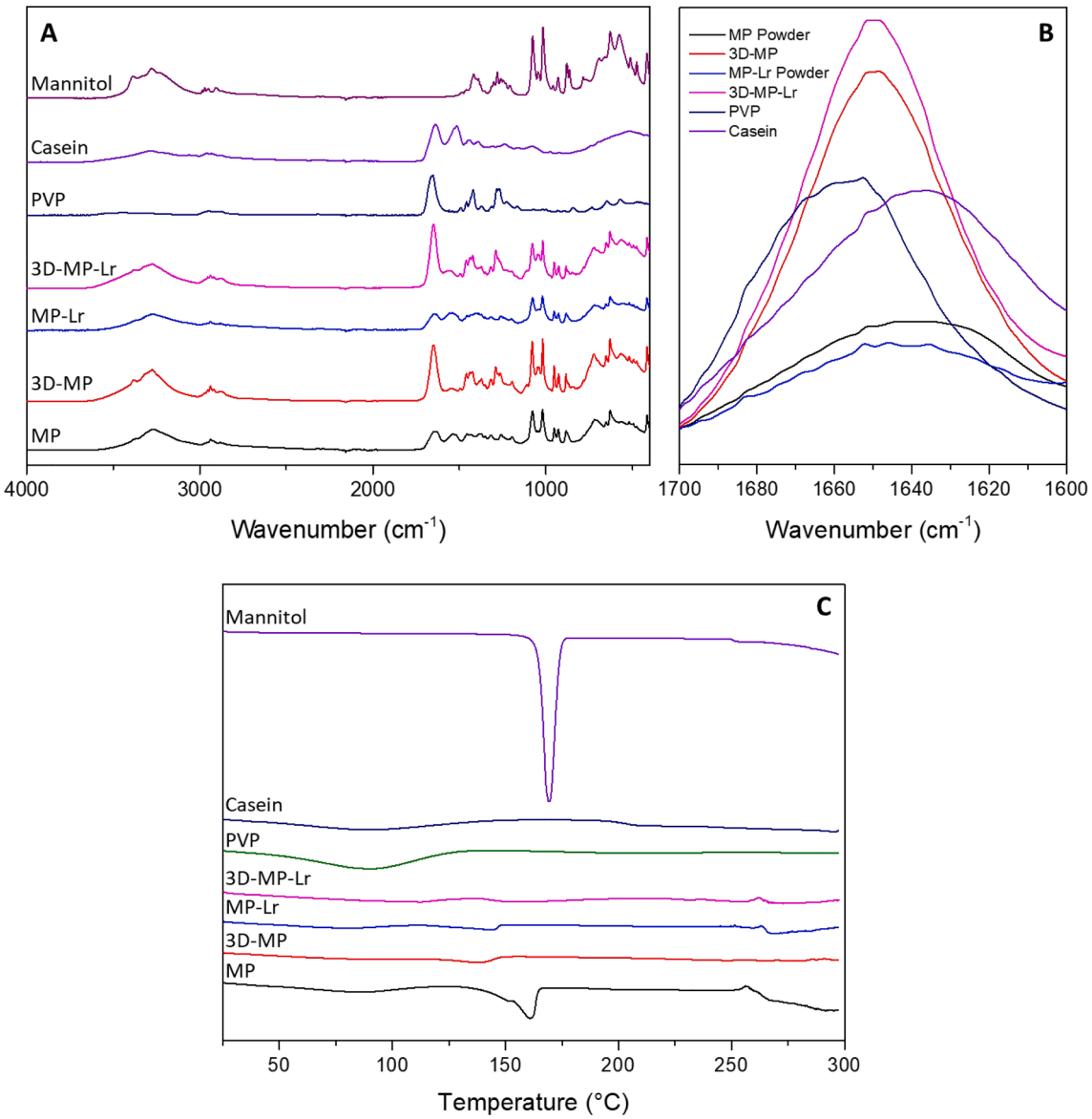

Fig. 6. FTIR spectra of 3D-MP, 3D-MP-Lr, MP, MP-Lr and the excipients used to prepare the printlet formulations (A). Magnified carbonyl region for the FTIR spectra (B). DSC curves of 3D-MP, 3D-MP-Lr, MP, MP-Lr and the excipients used to prepare the printlet formulations (C).

Table 3
Bacterial quantification and viability of non-encapsulated and encapsulated *Lr*, before and after being 3D printed. Data expressed as mean ± SD (n > 3).

	Initial log (CFU/g)	Final log (CFU/g)	Log reduction
3D-Lr	8.52 ± 0.01	5.47 ± 0.24	3.05
3D-MP-Lr	7.86 ± 0.03	7.34 ± 0.38	0.52

During the characterisation it was seen that the hardness of the printlets developed here were higher than the one reported for similar printlets (ca. 170 vs. 25–80 N) (Khaled et al., 2018b, 2018a). Interestingly, the printlets described in the literature were obtained through a similar robocasting 3D-printing using pastes loaded with pharmaceutical excipients. In those cases printlets contained high drug loadings and around 80% of the dry weight of the printlet was drug (paracetamol). In the present work printlets are prepared using high amounts of PVP plastisised with glycerol and therefore it is expected that they show higher mechanical resistance. The mechanical resistance seems to be related with relatively high disintegration times. These printlets described in this work showed longer disintegration times than 3D-printed obtained using a similar approach (Khaled et al., 2018b, 2018a). As mentioned earlier, these tablets were formulated containing high drug loading as opposed to the formulations described in this work. However, in all cases disintegration time was lower than 2 h. This indicate that the printlets will disperse within the stomach after administration. Moreover, the encapsulation of the probiotic bacteria will provide protection from the harsh conditions of the stomach as reported previously.

In addition to the characterisation results, viability studies were performed to ascertain if the probiotic bacteria were affected by the printing process. The results suggested that the probiotic bacteria survived the printing process maintaining its viability (Table 3). Interestingly, the encapsulation process is critical to ensure that, as when printlets were prepared, bacterial viability is maintained. Free bacterial showed a reduction of three CFU logs after the printing process. Moreover, particles did not show any significant aggregation during the printing process as after desegregating the printlets, the obtained particle sizes were equivalent to the initial ones. This was achieved by using a highly water soluble polymer such as PVP. This polymer has been used previously in the formulation of 3D printed tablets as binder (Khaled

et al., 2018b). In that work the resulting printlets showed fast dissolution kinetics (ca. 1 min). The results reported in this paper showed that PVP yielded homogeneous materials and that it forms H-bonds with the caseinate formulation. The presence of these interactions and the higher PVP content than in previously reported works yielded longer disintegration times. However, the disintegration times were under 2 h and therefore the resulting printlets can be easily dispersed within the stomach. Additionally, previous reports of casein-based microparticles suggest that after dispersion casein-based microparticles tend to reach distal areas of the intestine and colon as they are not mucoadhesive (Peñalva et al., 2023).

The present work offers advantages over previously published methods for 3D-printing of probiotics, as the methods described previously required formulations containing several components (Kuo et al., 2022; Yoha et al., 2021). The formulations described here only requires PVP and a small amount of glycerol as a plastisiser. This excipient is required as otherwise PVP-based printlets showed cracks during the drying process.

These results are encouraging as they highlight the versatility of 3D-printing as a tool to manufacture not only pharmaceutical formulations but to prepare formulations loaded with live bacteria. Finally, it is important to note that the technology developed here can be applied to 3D-printing of food adding probiotic bacteria. This is especially interesting considering that the global market value for 3D-printed food is projected to grow from 226.2 million of USD in 2021 up until 15.1 billion of USD by 2031 (Aniket K, n.d.; MBI Research, 2023; Polaris Market Research, 2022; Tong et al., 2021).

CRediT authorship contribution statement

Pablo Rosas-Val: Conceptualization, Methodology, Data curation, Investigation, Formal analysis, Writing – original draft. **Masoud Adhami:** Methodology, Data curation, Investigation, Formal analysis. **Ana Brotons-Canto:** Writing – review & editing, Supervision. **Carlos Gamazo:** Writing – review & editing, Supervision. **Juan M. Irache:** Conceptualization, Resources. **Eneko Larrañeta:** Conceptualization, Methodology, Data curation, Investigation, Resources, Formal analysis, Writing – original draft.

Declaration of Competing Interest

The authors declare that they have no known competing financial interests or personal relationships that could have appeared to influence the work reported in this paper.

Data availability

The authors are unable or have chosen not to specify which data has been used.

Acknowledgments

This work was financially supported by the Wellcome Trust (UNS40040) and Gobierno de Navarra, Spain (Research projects in health sciences 2023 ref. 642541).

References

Agüeros, M., Esparza, I., Gamazo, C., González-Ferrero, C., González-Navarro, C., Irache, J.M., Penalva, R., Romo, A., Virto, R., 2013. Microparticles for encapsulating probiotics, production and uses thereof. EP2868206A2.

Ahuja, Kunal, Bayas, Sarita, n.d. Probiotics Market Size, COVID-19 Impact Analysis, Regional Outlook, Growth Potential, Competitive Market Share & Forecast, 2023 – 2032 [WWW Document]. Global Market Insights. https://www.gminsights.com/industry-analysis/probiotics-market (accessed 3.7.23).

Aniket K, R.D., n.d. Food 3D Printing Market by Ingredient (Dough, Fruits and vegetables, Proteins, Sauces, Dairy Products, Carbohydrates, Others), by End User (Government, Commercial, Residential), by Technologies (Extrusion-based printing, Binder jetting, Selective laser sintering, Inkjet printing): Global Opportunity Analysis and Industry Forecast, 2021-2031 [WWW Document]. https://www.alliedmarketresearch.com/food-3d-printing-market-A08587 (accessed 3.10.22).

Arafat, B., Qinna, N., Cieszynska, M., Forbes, R.T., Alhnan, M.A., 2018. Tailored on demand anti-coagulant dosing: an in vitro and in vivo evaluation of 3D printed purpose-designed oral dosage forms. Eur. J. Pharm. Biopharm. 128, 282–289. https://doi.org/10.1016/j.ejpb.2018.04.010.

Awad, A., Fina, F., Trenfield, S., Patel, P., Goyanes, A., Gaisford, S., Basit, A., 2019. 3D printed pellets (miniprintlets): a novel, multi-drug, controlled release platform technology. Pharmaceutics 11, 148. https://doi.org/10.3390/pharmaceutics11040148.

Baiano, A., 2022. 3D printed foods: a comprehensive review on technologies, nutritional value, safety, consumer attitude, regulatory framework, and economic and sustainability issues. Food Rev. Intl. 38, 986–1016. https://doi.org/10.1080/87559129.2020.1762091.

Bermudez-Brito, M., Muñoz-Quezada, S., Gomez-Llorente, C., Romero, F., Gil, A., 2014. *Lactobacillus rhamnosus* and its cell-free culture supernatant differentially modulate inflammatory biomarkers in *Escherichia coli* -challenged human dendritic cells. Br. J. Nutr. 111, 1727–1737. https://doi.org/10.1017/S0007114513004303.

Cell Biotech., Co.L., 2023. Probiotics DUOLAC [WWW Document]. https://www.duolac.com/worldwide-patented-dual-coating-technology/ (accessed 4.20.23).

Bruni, G., Berbenni, V., Milanese, C., Girella, A., Cofrancesco, P., Bellazzi, G., Marini, A., 2009. Physico-chemical characterization of anhydrous D-mannitol. J. Therm. Anal. Calorim. 95, 871–876. https://doi.org/10.1007/s10973-008-9384-5.

Can Karaca, A., Low, N.H., Nickerson, M.T., 2015. Potential use of plant proteins in the microencapsulation of lipophilic materials in foods. Trends Food Sci. Technol. 42, 5–12. https://doi.org/10.1016/j.tifs.2014.11.002.

Chan, S.-Y., Chung, Y.-Y., Cheah, X.-Z., Tan, E.-Y.-L., Quah, J., 2015. The characterization and dissolution performances of spray dried solid dispersion of ketoprofen in hydrophilic carriers. Asian J. Pharm. Sci. 10, 372–385. https://doi.org/10.1016/j.ajps.2015.04.003.

Cukrowska, B., Ceregra, A., Maciorkowska, E., Surowska, B., Zegadło-Mylik, M.A., Konopka, E., Trojanowska, I., Zakrzewska, M., Bierła, J.B., Zakrzewski, M., Kanarek, E., Motyl, I., 2021. The Effectiveness of probiotic *Lactobacillus rhamnosus* and *Lactobacillus casei* strains in children with atopic dermatitis and cow's milk protein allergy: a multicenter, randomized, double blind. Placebo Controlled Study. Nutrients 13, 1169. https://doi.org/10.3390/nu13041169.

Dioso, C.M., Vital, P., Arellano, K., Park, H., Todorov, S.D., Ji, Y., Holzapfel, W., 2020. Do your kids get what you paid for? Evaluation of commercially available probiotic products intended for children in the Republic of the Philippines and the Republic of Korea. Foods 9, 1229. https://doi.org/10.3390/foods9091229.

Dodoo, C.C., Stapleton, P., Basit, A.W., Gaisford, S., 2020. The potential of Streptococcus salivarius oral films in the management of dental caries: an inkjet printing approach. Int. J. Pharm. 591, 119962 https://doi.org/10.1016/j.ijpharm.2020.119962.

Dou, X., Qiao, L., Chang, J., Yan, S., Song, X., Chen, Y., Xu, Q., Xu, C., 2021. *Lactobacillus casei* ATCC 393 and it's metabolites alleviate dextran sulphate sodium-induced ulcerative colitis in mice through the NLRP3-(Caspase-1)/IL-1β pathway. Food Funct. 12, 12022–12035. https://doi.org/10.1039/D1FO02405A.

España, H., 2023. Laboratorios Heel España lanza al mercado Gasteel, Gasteel Kid y Gasteel Plus, los nuevos simbióticos de la línea HeelProbiotics [WWW Document]. accessed 4.2.23. https://www.heel.es/es/laboratorios-heel-espana-lanza-al-mercado-gasteel-gasteel-kid-y-gasteel-plus-los-nuevos-simbioticos-de-la-l%C3%ADnea-heelprobiotics.html.

FAO/WHO, 2006. Probiotics in Food Health and nutritional properties and guidelines for evaluation. FAO Food Nutr. Pap.

Fiore, W., Arioli, S., Guglielmetti, S., 2020. The neglected microbial components of commercial probiotic formulations. Microorganisms 8, 1177. https://doi.org/10.3390/microorganisms8081177.

Fonollá, J., Gracián, C., Maldonado-Lobón, J.A., Romero, C., Bédmar, A., Carrillo, J.C., Martín-Castro, C., Cabrera, A.L., García-Curiel, J.M., Rodríguez, C., Sanbonmatsu, S., Pérez-Ruiz, M., Navarro, J.M., Olivares, M., 2019. Effects of *Lactobacillus coryniformis* K8 CECT5711 on the immune response to influenza vaccination and the assessment of common respiratory symptoms in elderly subjects: a randomized controlled trial. Eur. J. Nutr. 58, 83–90. https://doi.org/10.1007/s00394-017-1573-1.

García-Segovia, P., García-Alcaraz, V., Balasch-Parisi, S., Martínez-Monzó, J., 2020. 3D printing of gels based on xanthan/konjac gums. Innov. Food Sci. Emerg. Technol. 64, 102343 https://doi.org/10.1016/j.ifset.2020.102343.

Goyanes, A., Scarpa, M., Kamlow, M., Gaisford, S., Basit, A.W., Orlu, M., 2017. Patient acceptability of 3D printed medicines. Int J Pharm 530, 71–78. https://doi.org/10.1016/j.ijpharm.2017.07.064.

Goyanes, A., Madla, C.M., Umerji, A., Duran Piñeiro, G., Giraldez Montero, J.M., Lamas Diaz, M.J., Gonzalez Barcia, M., Taherali, F., Sánchez-Pintos, P., Couce, M.-L., Gaisford, S., Basit, A.W., 2019. Automated therapy preparation of isoleucine formulations using 3D printing for the treatment of MSUD: first single-centre, prospective, crossover study in patients. Int. J. Pharm. 567, 118497 https://doi.org/10.1016/j.ijpharm.2019.118497.

Gültekin, H.E., Tort, S., Tuğcu-Demiröz, F., Acartürk, F., 2021. 3D printed extended release tablets for once daily use: an *in vitro* and in vivo evaluation study for a personalized solid dosage form. Int. J. Pharm. 596, 120222 https://doi.org/10.1016/j.ijpharm.2021.120222.

Hill, C., Guarner, F., Reid, G., Gibson, G.R., Merenstein, D.J., Pot, B., Morelli, L., Canani, R.B., Flint, H.J., Salminen, S., Calder, P.C., Sanders, M.E., 2014. The International Scientific Association for Probiotics and Prebiotics consensus statement on the scope and appropriate use of the term probiotic. Nat. Rev. Gastroenterol. Hepatol. 11, 506–514. https://doi.org/10.1038/nrgastro.2014.66.

Kadry, H., Al-Hilal, T.A., Keshavarz, A., Alam, F., Xu, C., Joy, A., Ahsan, F., 2018. Multi-purposable filaments of HPMC for 3D printing of medications with tailored drug release and timed-absorption. Int. J. Pharm. 544, 285–296. https://doi.org/10.1016/j.ijpharm.2018.04.010.

Khaled, S.A., Alexander, M.R., Irvine, D.J., Wildman, R.D., Wallace, M.J., Sharpe, S., Yoo, J., Roberts, C.J., 2018a. Extrusion 3D printing of paracetamol tablets from a single formulation with tunable release profiles through control of tablet geometry. AAPS PharmSciTech 19, 3403–3413. https://doi.org/10.1208/s12249-018-1107-z.

Khaled, S.A., Alexander, M.R., Wildman, R.D., Wallace, M.J., Sharpe, S., Yoo, J., Roberts, C.J., 2018b. 3D extrusion printing of high drug loading immediate release paracetamol tablets. Int. J. Pharm. 538, 223–230. https://doi.org/10.1016/j.ijpharm.2018.01.024.

Kollamaram, G., Croker, D.M., Walker, G.M., Goyanes, A., Basit, A.W., Gaisford, S., 2018. Low temperature fused deposition modeling (FDM) 3D printing of thermolabile drugs. Int. J. Pharm. 545, 144–152. https://doi.org/10.1016/j.ijpharm.2018.04.055.

Kouzani, A.Z., Adams, S., J. Whyte, D., Oliver, R., Hemsley, B., Palmer, S., Balandin, S., 2017. 3D Printing of food for people with swallowing difficulties. KnE Eng. 2, 23. 10.18502/keg.v2i2.591.

Kowalczuk, P.B., Drzymala, J., 2016. Physical meaning of the Sauter mean diameter of spherical particulate matter. Part. Sci. Technol. 34, 645–647. https://doi.org/10.1080/02726351.2015.1099582.

Kuo, S.W., Chang, F.C., 2001. Studies of miscibility behavior and hydrogen bonding in blends of poly(vinylphenol) and poly(vinylpyrrolidone). Macromolecules 34, 5224–5228. https://doi.org/10.1021/ma010517a.

Kuo, C.-C., Clark, S., Qin, H., Shi, X., 2022. Development of a shelf-stable, gel-based delivery system for probiotics by encapsulation, 3D printing, and freeze-drying. LWT 157, 113075. https://doi.org/10.1016/j.lwt.2022.113075.

Lallemand Inc, 2023. Protective Technologies [WWW Document]. accessed 4.20.23. https://lallemand-health-solutions.com/en/process/technologies/.

Liu, Z., Bhandari, B., Prakash, S., Mantihal, S., Zhang, M., 2019. Linking rheology and printability of a multicomponent gel system of carrageenan-xanthan-starch in extrusion based additive manufacturing. Food Hydrocoll. 87, 413–424. https://doi.org/10.1016/j.foodhyd.2018.08.026.

Liu, Z., Bhandari, B., Zhang, M., 2020. Incorporation of probiotics (<i>Bifidobacterium animalis<i> subsp. *Lactis*) into 3D printed mashed potatoes: effects of variables on the viability. Food Res. Int. 128, 108795 https://doi.org/10.1016/j.foodres.2019.108795.

Lundelin, K., Poussa, T., Salminen, S., Isolauri, E., 2017. Long-term safety and efficacy of perinatal probiotic intervention: evidence from a follow-up study of four randomized, double-blind, placebo-controlled trials. Pediatr. Allergy Immunol. 28, 170–175. https://doi.org/10.1111/pai.12675.

Maldonado Galdeano, C., Cazorla, S.I., Lemme Dumit, J.M., Vélez, E., Perdigón, G., 2019. Beneficial effects of probiotic consumption on the immune system. Ann. Nutr. Metab. 74, 115–124. https://doi.org/10.1159/000496426.

Malebari, A.M., Kara, A., Khayyat, A.N., Mohammad, K.A., Serrano, D.R., 2022. Development of advanced 3D-printed solid dosage pediatric formulations for HIV treatment. Pharmaceuticals 15, 435. https://doi.org/10.3390/ph15040435.

Martin, N.K., Domínguez-Robles, J., Stewart, S.A., Cornelius, V.A., Anjani, Q.K., Utomo, E., García-Romero, I., Donnelly, R.F., Margariti, A., Lamprou, D.A., Larrañeta, E., 2021. Fused deposition modelling for the development of drug loaded cardiovascular prosthesis. Int. J. Pharm. 595, 120243 https://doi.org/10.1016/j.ijpharm.2021.120243.

Martinez, P.R., Goyanes, A., Basit, A.W., Gaisford, S., 2018. Influence of geometry on the drug release profiles of stereolithographic (SLA) 3D-printed tablets. AAPS PharmSciTech 19, 3355–3361. https://doi.org/10.1208/s12249-018-1075-3.

Mazziotta, C., Tognon, M., Martini, F., Torreggiani, E., Rotondo, J.C., 2023. Probiotics mechanism of action on immune cells and beneficial effects on human health. Cells 12, 184. https://doi.org/10.3390/cells12010184.

MBI Research, 2023. 3D Food Printing Market By Ingredient (Fruits & Vegetables, Proteins, Dairy Products, Dough, Carbohydrates, and Others) By End-User (Commercial and Residential (Restaurants, Confectioneries, Bakeries, and Others)) Forecast Period 2022-2030.

Munir, M., Kett, V.L., Dunne, N.J., McCarthy, H.O., 2022. Development of a spray-dried formulation of peptide-DNA nanoparticles into a dry powder for pulmonary delivery using factorial design. Pharm. Res. 39, 1215–1232. https://doi.org/10.1007/s11095-022-03256-4.

Muñoz-Quezada, S., Chenoll, E., María Vieites, J., Genovés, S., Maldonado, J., Bermúdez-Brito, M., Gomez-Llorente, C., Matencio, E., José Bernal, M., Romero, F., Suárez, A., Ramón, D., Gil, A., 2013b. Isolation, identification and characterisation of three novel probiotic strains (*Lactobacillus paracasei* CNCM I-4034, *Bifidobacterium breve* CNCM I-4035 and *Lactobacillus rhamnosus* CNCM I-4036) from the faeces of exclusively breast-fed infants. Br. J. Nutr. 109, S51–S62. https://doi.org/10.1017/S0007114512005211.

Muñoz-Quezada, S., Bermudez-Brito, M., Chenoll, E., Genovés, S., Gomez-Llorente, C., Plaza-Diaz, J., Matencio, E., José Bernal, M., Romero, F., Ramón, D., Gil, A., 2013a. Competitive inhibition of three novel bacteria isolated from faeces of breast milk-fed infants against selected enteropathogens. Brit. J. Nutr. 109, S63–S69. 10.1017/S0007114512005600.

Naissinger da Silva, M., Tagliapietra, B.L., Flores, V. do A., Pereira dos Santos Richards, N.S., 2021. In vitro test to evaluate survival in the gastrointestinal tract of commercial probiotics. Curr. Res. Food Sci. 4, 320–325. 10.1016/j.crfs.2021.04.006.

National Institute of Helath, 2022. Probiotics [WWW Document]. accessed 5.10.23. https://ods.od.nih.gov/factsheets/Probiotics-HealthProfessional/.

Pan, K., Zhong, Q., Baek, S.J., 2013. Enhanced dispersibility and bioactivity of curcumin by encapsulation in casein nanocapsules. J. Agric. Food Chem. 61, 6036–6043. https://doi.org/10.1021/jf400752a.

Pant, A., Lee, A.Y., Karyappa, R., Lee, C.P., An, J., Hashimoto, M., Tan, U.-X., Wong, G., Chua, C.K., Zhang, Y., 2021. 3D food printing of fresh vegetables using food hydrocolloids for dysphagic patients. Food Hydrocoll. 114, 106546 https://doi.org/10.1016/j.foodhyd.2020.106546.

Patro, J.N., Ramachandran, P., Barnaba, T., Mammel, M.K., Lewis, J.L., Elkins, C.A., 2016. Culture-independent metagenomic surveillance of commercially available probiotics with high-throughput next-generation sequencing. mSphere 1. 10.1128/mSphere.00057-16.

Penalva, R., Esparza, I., Larraneta, E., González-Navarro, C.J., Gamazo, C., Irache, J.M., 2015. Zein-based nanoparticles improve the oral bioavailability of resveratrol and its anti-inflammatory effects in a mouse model of endotoxic shock. J. Agric. Food Chem. 63, 5603–5611. https://doi.org/10.1021/jf505694e.

Peñalva, R., Esparza, I., Morales-Gracia, J., González-Navarro, C.J., Larrañeta, E., Irache, J.M., 2019. Casein nanoparticles in combination with 2-hydroxypropyl-β-cyclodextrin improves the oral bioavailability of quercetin. Int. J. Pharm. 570, 118652 https://doi.org/10.1016/j.ijpharm.2019.118652.

Peñalva, R., Martínez-López, A.L., Gamazo, C., Gonzalez-Navarro, C.J., González-Ferrero, C., Virto-Resano, R., Brotons-Canto, A., Vitas, A.I., Collantes, M., Peñuelas, I., Irache, J.M., 2023. Encapsulation of *Lactobacillus plantarum* in casein-chitosan microparticles facilitates the arrival to the colon and develops an immunomodulatory effect. Food Hydrocoll. 136, 108213 https://doi.org/10.1016/j.foodhyd.2022.108213.

Peng, X., Ed-Dra, A., Song, Y., Elbediwi, M., Nambiar, R.B., Zhou, X., Yue, M., 2022. *Lacticaseibacillus rhamnosus* alleviates intestinal inflammation and promotes microbiota-mediated protection against Salmonella fatal infections. Front. Immunol. 13. 10.3389/fimmu.2022.973224.

Picco, C.J., Utomo, E., McClean, A., Domínguez-Robles, J., Anjani, Q.K., Volpe-Zanutto, F., McKenna, P.E., Acheson, J.G., Malinova, D., Donnelly, R.F., Larrañeta, E., 2023. Development of 3D-printed subcutaneous implants using concentrated polymer/drug solutions. Int. J. Pharm. 631, 122477 https://doi.org/10.1016/j.ijpharm.2022.122477.

Plaza-Diaz, J., Gomez-Llorente, C., Campaña-Martin, L., Matencio, E., Ortuño, I., Martínez-Silla, R., Gomez-Gallego, C., Periago, M.J., Ros, G., Chenoll, E., Genovés, S., Casinos, B., Silva, Á., Corella, D., Portolés, O., Romero, F., Ramón, D., Perez de la Cruz, A., Gil, A., Fontana, L., 2013. Safety and immunomodulatory effects of three probiotic strains isolated from the feces of breast-fed infants in healthy adults: SETOPROB study. PLoS One 8, e78111.

Polaris Market Research, 2022. 3D Food printing market share, size, trends, industry analysis report by Ingredient (dough, carbohydrates, proteins, sauces, dairy products, fruits & vegetables, others); by vertical; by technology; by region. Segment Forecast 2022–2030.

Prakash, S., 2008. Colon-targeted delivery of live bacterial cell biotherapeutics including microencapsulated live bacterial cells. Biologics 355. https://doi.org/10.2147/BTT.S2372.

Quintero Quiroz, J., Velazquez, V., Corrales-Garcia, L.L., Torres, J.D., Delgado, E., Ciro, G., Rojas, J., 2020. Use of plant proteins as microencapsulating agents of bioactive compounds extracted from annatto seeds (*Bixa orellana* L.). Antioxidants 9, 310. https://doi.org/10.3390/antiox9040310.

Robles-Martinez, P., Xu, X., Trenfield, S.J., Awad, A., Goyanes, A., Telford, R., Basit, A.W., Gaisford, S., 2019. 3D printing of a multi-layered polypill containing six drugs using a novel stereolithographic method. Pharmaceutics 11, 274. https://doi.org/10.3390/pharmaceutics11060274.

Sanchez, M., Darimont, C., Drapeau, V., Emady-Azar, S., Lepage, M., Rezzonico, E., Ngom-Bru, C., Berger, B., Philippe, L., Ammon-Zuffrey, C., Leone, P., Chevrier, G., St-Amand, E., Marette, A., Doré, J., Tremblay, A., 2014. Effect of *Lactobacillus rhamnosus* CGMCC1.3724 supplementation on weight loss and maintenance in obese men and women. Br. J. Nutr. 111, 1507–1519. https://doi.org/10.1017/S0007114513003875.

Sang, Y., Wang, J., Zhang, Y., Gao, H., Ge, S., Feng, H., Zhang, Y., Ren, F., Wen, P., Wang, R., 2023. Influence of temperature during freeze-drying process on the viability of *Bifidobacterium longum* BB68S. Microorganisms 11, 181. https://doi.org/10.3390/microorganisms11010181.

Santivarangkna, C., Kulozik, U., Foerst, P., 2008. Inactivation mechanisms of lactic acid starter cultures preserved by drying processes. J. Appl. Microbiol. 105, 1–13. https://doi.org/10.1111/j.1365-2672.2008.03744.x.

Segers, M.E., Lebeer, S., 2014. Towards a better understanding of *Lactobacillus rhamnosus* GG - host interactions. Microb. Cell Fact. 13, S7. https://doi.org/10.1186/1475-2859-13-S1-S7.

Silva, I.A., Lima, A.L., Gratieri, T., Gelfuso, G.M., Sa-Barreto, L.L., Cunha-Filho, M., 2022. Compatibility and stability studies involving polymers used in fused deposition modeling 3D printing of medicines. J. Pharm. Anal. 12, 424–435. https://doi.org/10.1016/j.jpha.2021.09.010.

Slykerman, R.F., Hood, F., Wickens, K., Thompson, J.M.D., Barthow, C., Murphy, R., Kang, J., Rowden, J., Stone, P., Crane, J., Stanley, T., Abels, P., Purdie, G., Maude, R., Mitchell, E.A., 2017. Effect of *Lactobacillus rhamnosus* HN001 in pregnancy on postpartum symptoms of depression and anxiety: a randomised double-blind placebo-controlled trial. EBioMedicine 24, 159–165. https://doi.org/10.1016/j.ebiom.2017.09.013.

Sohn, M., Jung, H., Lee, W.S., Kim, T.H., Lim, S., 2023. Effect of *Lactobacillus plantarum* LMT1-48 on body fat in overweight subjects: a randomized, double-blind, placebo-controlled trial. Diabetes Metab. J. 47, 92–103. https://doi.org/10.4093/dmj.2021.0370.

Stasiak-Różańska, L., Berthold-Pluta, A., Pluta, A.S., Dasiewicz, K., Garbowska, M., 2021. Effect of simulated gastrointestinal tract conditions on survivability of probiotic bacteria present in commercial preparations. Int. J. Environ. Res. Public Health 18, 1108. https://doi.org/10.3390/ijerph18031108.

Stewart, S.A., Domínguez-Robles, J., McIlorum, V.J., Gonzalez, Z., Utomo, E., Mancuso, E., Lamprou, D.A., Donnelly, R.F., Larrañeta, E., 2020. Poly(caprolactone)-based coatings on 3D-printed biodegradable implants: a novel strategy to prolong delivery of hydrophilic drugs. Mol. Pharm. 17, 3487–3500. https://doi.org/10.1021/acs.molpharmaceut.0c00515.

Sun, N., Liang, Y., Yu, B., Tan, C., Cui, B., 2016. Interaction of starch and casein. Food Hydrocoll, 60, 572–579. https://doi.org/10.1016/j.foodhyd.2016.04.029.

Szajewska, H., Skórka, A., Ruszczyński, M., Gieruszczak-Białek, D., 2013. Meta-analysis: *Lactobacillus* GG for treating acute gastroenteritis in children - updated analysis of randomised controlled trials. Aliment Pharmacol. Ther. 38, 467–476. https://doi.org/10.1111/apt.12403.

Tekko, I.A., Chen, G., Domínguez-Robles, J., Thakur, R.R.S., Hamdan, I.M.N., Vora, L., Larrañeta, E., McElnay, J.C., McCarthy, H.O., Rooney, M., Donnelly, R.F., 2020. Development and characterisation of novel poly (vinyl alcohol)/poly (vinyl pyrrolidone)-based hydrogel-forming microneedle arrays for enhanced and sustained transdermal delivery of methotrexate. Int. J. Pharm. 586, 119580 https://doi.org/10.1016/j.ijpharm.2020.119580.

Temple, N.J., 2022. A rational definition for functional foods: a perspective. Front. Nutr. 9 https://doi.org/10.3389/fnut.2022.957516.

Terpou, A., Papadaki, A., Lappa, I., Kachrimanidou, V., Bosnea, L., Kopsahelis, N., 2019. Probiotics in food systems: significance and emerging strategies towards improved viability and delivery of enhanced beneficial value. Nutrients 11, 1591. https://doi.org/10.3390/nu11071591.

Tong, A., Pham, Q.L., Abatemarco, P., Mathew, A., Gupta, D., Iyer, S., Voronov, R., 2021. Review of low-cost 3D bioprinters: state of the market and observed future trends. SLAS Technol. 26, 333–366. https://doi.org/10.1177/24726303211020297.

Ullah, M., Raza, A., Ye, L., Yu, Z., 2019. Viability and composition validation of commercial probiotic products by selective culturing combined with next-generation sequencing. Microorganisms 7, 188. https://doi.org/10.3390/microorganisms7070188.

Utomo, E., Domínguez-Robles, J., Anjani, Q.K., Picco, C.J., Korelidou, A., Magee, E., Donnelly, R.F., Larrañeta, E., 2023. Development of 3D-printed vaginal devices containing metronidazole for alternative bacterial vaginosis treatment. Int. J. Pharm. X 5, 100142. https://doi.org/10.1016/j.ijpx.2022.100142.

Varghese, R., Sood, P., Salvi, S., Karsiya, J., Kumar, D., 2022. 3D printing in the pharmaceutical sector: advances and evidences. Sensors Int. 3, 100177 https://doi.org/10.1016/j.sintl.2022.100177.

Vecchione, A., Celandroni, F., Mazzantini, D., Senesi, S., Lupetti, A., Ghelardi, E., 2018. Compositional quality and potential gastrointestinal behavior of probiotic products commercialized in Italy. Front. Med. (Lausanne) 5. https://doi.org/10.3389/fmed.2018.00059.

Vinderola, C.G., Reinheimer, J.A., 2003. Lactic acid starter and probiotic bacteria: a comparative "in vitro" study of probiotic characteristics and biological barrier resistance. Food Res. Int. 36, 895–904. https://doi.org/10.1016/S0963-9969(03)00098-X.

Vivek, K., Mishra, S., Pradhan, R.C., Nagarajan, M., Kumar, P.K., Singh, S.S., Manvi, D., Gowda, N.N., 2023. A comprehensive review on microencapsulation of probiotics: technology, carriers and current trends. Appl. Food Res. 3, 100248 https://doi.org/10.1016/j.afres.2022.100248.

Wang, Y., He, Y., Liang, Y., Liu, H., Chen, X., Kulyar, M.-F.-A., Shahzad, A., Wei, K., Li, K., 2023. Fecal microbiota transplantation attenuates *Escherichia coli* infected outgrowth by modulating the intestinal microbiome. Microb. Cell Fact. 22, 30. https://doi.org/10.1186/s12934-023-02027-z.

Wang, G.-Q., Pu, J., Yu, X.-Q., Xia, Y.-J., Ai, L.-Z., 2020. Influence of freezing temperature before freeze-drying on the viability of various *Lactobacillus plantarum* strains. J. Dairy Sci. 103, 3066–3075. https://doi.org/10.3168/jds.2019-17685.

Xu, D., Liu, Z., An, Z., Hu, L., Li, H., Mo, H., Hati, S., 2023. Incorporation of probiotics into 3D printed Pickering emulsion gel stabilized by tea protein/xanthan gum. Food Chem. 409, 135289 https://doi.org/10.1016/j.foodchem.2022.135289.

Yamanbaeva, G., Schaub, A.-C., Schneider, E., Schweinfurth, N., Kettelhack, C., Doll, J.P. K., Mählmann, L., Brand, S., Beglinger, C., Borgwardt, S., Lang, U.E., Schmidt, A., 2023. Effects of a probiotic add-on treatment on fronto-limbic brain structure, function, and perfusion in depression: secondary neuroimaging findings of a randomized controlled trial. J. Affect. Disord. 324, 529–538. https://doi.org/10.1016/j.jad.2022.12.142.

Yoha, K.S., Anukiruthika, T., Anila, W., Moses, J.A., Anandharamakrishnan, C., 2021. 3D printing of encapsulated probiotics: Effect of different post-processing methods on the stability of *Lactiplantibacillus plantarum* (NCIM 2083) under static *in vitro* digestion conditions and during storage. LWT 146, 111461. https://doi.org/10.1016/j.lwt.2021.111461.

Zawistowska-Rojek, A., Zaręba, T., Tyski, S., 2022. Microbiological testing of probiotic preparations. Int. J. Environ. Res. Public Health 19, 5701. https://doi.org/10.3390/ijerph19095701.

Zhao, T., Liu, F., Duan, X., Xiao, C., Liu, X., 2018. Physicochemical properties of lutein-loaded microcapsules and their uptake via Caco-2 monolayers. Molecules 23, 1805. https://doi.org/10.3390/molecules23071805.

Zheng, Z., Lv, J., Yang, W., Pi, X., Lin, W., Lin, Z., Zhang, W., Pang, J., Zeng, Y., Lv, Z., Lao, H., Chen, Y., Yang, F., 2020. Preparation and application of subdivided tablets using 3D printing for precise hospital dispensing. Eur. J. Pharm. Sci. 149, 105293 https://doi.org/10.1016/j.ejps.2020.105293.